Optical signature of Mg-doped GaN: Transfer processes

G. Callsen,* M. R. Wagner, T. Kure, J. S. Reparaz, M. Bügler, J. Brunnmeier, C. Nenstiel, and A. Hoffmann
Institut für Festkörperphysik, Technische Universität Berlin, Hardenbergstr. 36, 10623 Berlin, Germany

M. Hoffmann, J. Tweedie, Z. Bryan, S. Aygun, R. Kirste, R. Collazo, and Z. Sitar
Material Science and Engineering, North Carolina State University, Raleigh, North Carolina, United States
(Received 14 June 2012; published 23 August 2012)

Mg doping of high quality, metal organic chemical vapor deposition grown GaN films results in distinct traces in their photoluminescence and photoluminescence excitation spectra. We analyze GaN:Mg grown on sapphire substrates and identify two Mg related acceptor states, one additional acceptor state and three donor states that are involved in the donor-acceptor pair band transitions situated at 3.26–3.29 eV in GaN:Mg. The presented determination of the donor-acceptor pair band excitation channels by photoluminescence excitation spectroscopy in conjunction with temperature-dependent photoluminescence measurements results in a direct determination of the donor and acceptor binding, localization, and activation energies, which is put into a broader context based on Haynes's rule. Furthermore, we analyze the biexponential decay dynamics of the photoluminescence signal of the acceptor and donor bound excitons. As all observed lifetimes scale with the localization energy of the donor and acceptor related bound excitons, defect and complex bound excitons can be excluded as their origin. Detailed analysis of the exciton transfer processes in the close energetic vicinity of the GaN band edge reveals excitation via free and bound excitonic channels but also via an excited state as resolved for the deepest localized Mg related acceptor bound exciton. For the two Mg acceptor states, we determine binding energies of 164 ± 5 and 195 ± 5 meV, which is in good agreement with recent density functional theory results. This observation confirms and quantifies the general dual nature of acceptor states in GaN based on the presented analysis of the photoluminescence and photoluminescence excitation spectra.

DOI: 10.1103/PhysRevB.86.075207 PACS number(s): 71.35.−y, 71.55.Eq, 78.55.Cr, 78.47.jd

I. INTRODUCTION

In recent years, the development of solid state light emitters for the blue to ultraviolet (UV) spectral range has caught rising interest, which naturally results in the task of bipolar doping of intermediate and wide band-gap materials like CdS,[1–3] ZnSe,[4] ZnO,[5–7] and GaN.[1,8] Up to date, only GaN and its ternary systems InGaN and AlGaN have matured towards technologically relevant applications as, e.g., blue and near UV light-emitting diodes[9,10] and blue laser diodes as originally invented by Nakamura *et al.*[11,12] While sufficient *n*-type conduction for light emitting devices was achieved in the early years of GaN growth, *p*-type doping with resulting predominant *p*-type conduction was an outstandingly challenging task until the breakthrough of Amano *et al.*[8] and Akasaki *et al.*[13] The first *p*-conducting GaN samples where doped with Mg and subsequently activated by low-energy electron beam irradiation (LEEBI) in order to remove the acceptor passivating hydrogen that originates from the metal organic chemical vapor deposition (MOCVD) growth procedure. In the following years, most relevant thermal annealing effects in order to remove the hydrogen[14] as well as photo-enhanced dissociation of Mg-H complexes[15,16] were extensively studied. As a result, a better understanding of the transition from highly resistive to well *p*-conductive GaN:Mg samples with hole concentrations in the mid 10^{17} cm^{-3} regime was achieved.

Despite the subsequent emergence of various optoelectronic devices, compensation mechanisms induced, e.g., by unintentional dopants and structural defects in *p*-doped GaN,[17,18] which still drastically limit today's device performance, have not been fully understood as in more matured systems such as ZnSe[19,20] or CdS.[2,3,21] Studying the luminescence traces of Mg-doped GaN with different compensation, doping and strain levels[22,23] has been proven as an effective tool for improving the growth procedures themselves but has also raised general questions concerning the twofold occurrence and stability[24] of acceptors in such wide band-gap materials. Rising interest in this dual nature of acceptors in GaN has just recently been triggered by publications of Monemar *et al.*[25] and Lany *et al.*[26] that led to novel insight concerning the general topic of acceptor doping in wide band-gap materials as also discussed by Gil *et al.*[1] for the case of CdS and GaN. Two Mg related acceptors were observed by photoluminescence (PL) spectroscopy[25] and assigned to one regular substitutional acceptor and one, under UV laser illumination unstable, Mg acceptor complex. Lyons *et al.*[27] theoretically described the Mg-H complex as possible origin for the observed instability of the related bound excitonic and donor-acceptor pair (DAP) band emission. However, the general dual nature of acceptor states in wide band-gap wurtzite materials like GaN,[1,26] CdS,[1] and ZnO[26] is a current topic of active debate[26,27] and requires still pending direct experimental confirmation with focus on the transfer processes which facilitate bound excitonic or DAP luminescences. Application of on-site hole state potentials[28] in density functional theory (DFT) calculations using the projector augmented wave method led to the prediction of a deep ground state (DGS) of the Mg acceptor in GaN (Mg_{Ga}) at 180 meV and a shallow transient Mg_{Ga} state (STS) at 150 meV relative to the valence band maximum.[26] Magnetic resonance studies by Glaser *et al.*[29,30] show the existence of such a deep, noneffective mass like Mg_{Ga} state, which coexists with a shallow and hence effective mass like Mg_{Ga} state in GaN. For the noneffective mass like DGS case, the acceptor wave

 ©2012 American Physical Society

function is mostly localized at a single N atom, whereas it is more delocalized for the effective mass like STS state,[28] which is the signature of a lattice relaxed deep and a shallow acceptor state. Both Mg_{Ga} related centers should participate in the frequently observed DAP emission of GaN:Mg, which can be shown by analyzing the carrier transfer processes via, e.g., photoluminescence excitation (PLE) spectroscopy. Also analyzing transfer processes in the close energetic vicinity of the GaN band edge will reveal strong differences for the excitation paths of, e.g., point defect/impurity bound excitons and complex bound excitons.[31] Deeply bound excitonic luminescence is a common PL trace in heteroepitaxially grown GaN[32] and hence must be distinguished from the relevant Mg_{Ga} bound excitons in order to facilitate consistent analysis by a combination of PLE, temperature dependent PL and time-resolved PL spectroscopy.[31]

In this work, we characterize donor and acceptor states in Mg-doped GaN by optical spectroscopy. These measurements do not only facilitate direct determination of crucial parameters such as binding (E_{bind}), localization (E_{loc}), and activation energies (E_{act}) but also support the active debate concerning the dual nature of Mg_{Ga} acceptor states in GaN.[26,27] We find acceptor binding energies of 164 ± 5 and 195 ± 5 meV for the STS and DGS Mg_{Ga} state, which is in good agreement with the theoretical values of Lany *et al*.[26] By analyzing the transfer processes based on PLE spectroscopy, we directly determine the donors and acceptors participating in the different DAP transitions. As a result, we obtain a precise determination of E_{bind} for all donor and acceptor states. The presented unique combination of PLE spectroscopy, temperature-dependent and time-resolved PL analysis allows us to distinguish between, e.g., complex and point defect bound excitons, DAP and (e, A) transitions, deep donor and shallow acceptor states and their related DAP luminescences. Evaluation of PLE spectra in the close energetic vicinity of the GaN band edge and its DAP luminescences reveals transfer processes originating from bound excitons, their excited states and the free A- and B-exciton that gives detailed insight into the nature of all observed luminescences with main focus on the dual nature of the Mg_{Ga} acceptor state in GaN.

II. EXPERIMENTAL DETAILS

In order to analyze as technologically relevant material as possible, we characterized heteroepitaxially MOCVD grown GaN:Mg. Our layers consist of a 700-nm-thick GaN:Mg layer deposited on a 1.3-μm-thick and not intentionally doped GaN buffer layer that was epitaxially grown on two-inch (0001) sapphire substrates.[33] The full set of specimens with a Mg doping concentration from 8×10^{17} to 2×10^{19} cm^{-3} was annealed under N_2 atmosphere at a temperature of 650 °C in order to remove passivating hydrogen.[14] The doping concentrations were determined based on the selected growth conditions, a method that was calibrated against secondary ion mass spectrometry data for specific samples. Thermal annealing was performed in a N_2 purged tube furnace for up to 2 hours. Continuous wave excitation for PL spectroscopy was achieved by a HeCd laser (325 nm), which excited the samples either in a helium bath (2 K) or closed-cycle helium cryostat for the temperature dependent PL measurements (3–300 K). Photoluminescence excitation (PLE) spectra were recorded using a dye laser (Coherent FL 3001, 20 ns pulse width, $\sim$5 μJ per pulse) that was tunable over the relevant spectral range from 3.2 to 3.6 eV. A XeCL-Excimer (Coherent, 308 nm, 100 Hz) laser was applied for optical pumping of the dye laser. As dyes we applied pure LC3400 (p-Terphenyl), LC3570 (BMQ), LC3590 (DMQ), LC3690 (QUI) in suitable solvents or customized dye mixtures in order to adopt the lasing range to the required PLE spectral range or to shift the wavelength of the background dye luminescence out of the spectral detection window. The spectral resolution of the excitation wavelength and the light dispersing 1 m additive double-monochromator (Spex 1701) was better than 50 μeV and all PLE spectra have been corrected for the wavelength-dependent individual dye efficiency. During recording of the PLE spectra the excitation power of the dye laser was constantly monitored and subsequently used to correct changes in the luminescence signal as induced by an altering excitation power. For time-resolved PL measurements we applied the fourth harmonic of a Nd:YAG laser at 266 nm (Coherent Antares 76s) with a pulse length of 60 ps and a subtractive 1-m double monochromator (Jarrell Ash, 25–100) with a resolution better than 100 μeV as a dispersing element. The PLE spectra were recorded using a bialkali photomultiplier tube (9789QB, EMI) in combination with a picoamperemeter and a damping low-pass filter as a detection system. The time-resolved PL measurements were performed with a bialkali multichannel plate detector (R3809U-52, Hamamatsu, transit-time spread below 30 ps) in conjunction with the single-photon counting technique.

III. DETERMINATION OF THE BINDING ENERGIES

Figure 1 shows the PL spectra of the GaN:Mg samples with different Mg concentration. In the not intentionally doped (NID) and the low Mg-doped samples (8×10^{17} to 2×10^{18} cm^{-3}) we observe the free A- and B-excitonic transitions (FXA, FXB). In the lowest Mg-doped sample (8×10^{17} cm^{-3}) such FXA and FXB luminescences appear at, e.g., 3.487 and 3.495 eV. Monemar *et al*. analyzed GaN:Mg grown by hydride vapor phase epitaxy (HVPE) in a comparably low Mg doping regime and obtained relaxed values for the free A- and B-excitonic transitions by PL spectroscopy at 3.478 and 3.484 eV.[34] The resulting energetic differences of 9 meV for the free A exciton and 11 meV for the free B exciton indicates compressive stress for the GaN:Mg layers due to the heteroepitaxial growth on sapphire as in the following briefly analyzed by support of Raman spectroscopy (not shown).

Two donor bound excitons (DBX2 and DBX3) dominate the spectra of the undoped and lowly Mg-doped samples with line positions at 3.480 and 3.474 eV. The donor bound exciton DBX1 at 3.483 eV is not well resolved in the PL spectra of Fig. 1 but appears as a trace in the PLE spectra of the lowest Mg-doped sample (8×10^{17} cm^{-3}) as shown in Figs. 2 and 8. With increasing Mg concentration in our samples, we observe more deeply bound excitons at 3.469, 3.457, and 3.445 eV, which are acceptor related as shown in this work and hence labeled as ABX1, ABX2, and ABX3. While ABX1 and ABX2 are already well noticeable in the PL spectra of the lowly Mg doped samples, we observe the

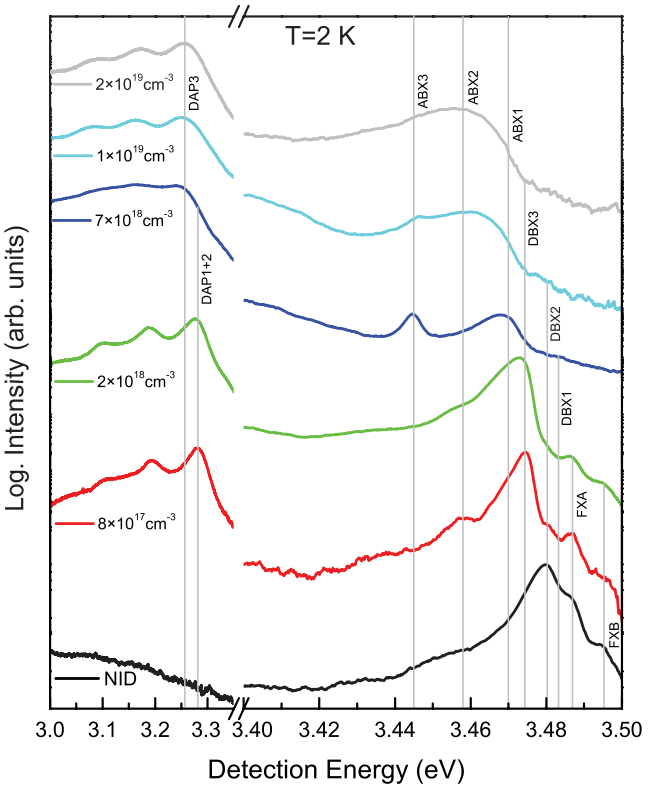

FIG. 1. (Color online) Low-temperature (2 K) PL spectra of not intentionally doped (NID) and fully thermally activated GaN:Mg samples with varying Mg content. The spectral range displays the full spectrum from the free excitons (FXA, FXB), over the donor and acceptor bound excitons (DBX, ABX), towards the spectral region of the donor-acceptor pair transitions (DAP).

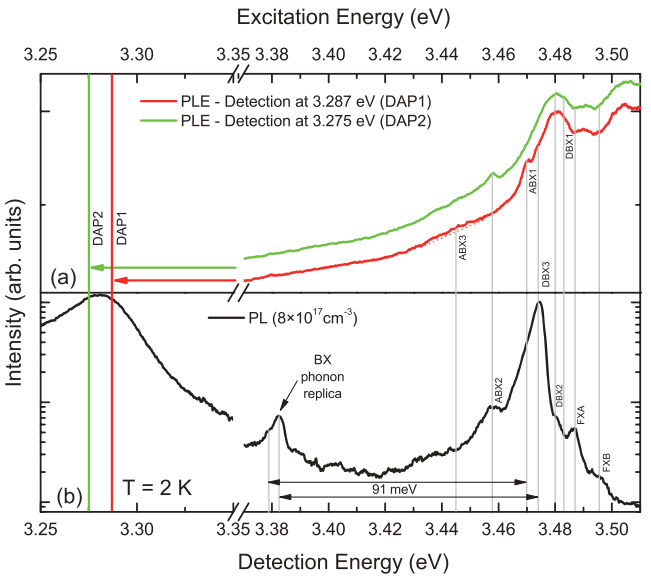

FIG. 2. (Color online) Low-temperature (2 K) PLE (a) and PL (b) spectra of a lowly doped (8×10^{17} cm^{-3}) and fully thermally activated GaN:Mg sample. PLE spectra with detection energies at the spectral positions of DAP1 and DAP2 reveal several excitation channels of the DAP that can be correlated to their corresponding PL transitions of the free excitons (FX) as well as donor (DBX) and acceptor (ABX) bound excitons.

clear appearance of the ABX3 transition at Mg concentrations of above 2×10^{18} cm^{-3}. The dominating donor-acceptor pair transition (DAP) in the doping regime with Mg concentrations below 10^{18} cm^{-3} is observed at an energy of 3.281 eV, which consists of two further spectral components as shown by PLE spectroscopy in Fig. 2 and is therefore labeled as DAP1 + 2. As soon as the Mg doping concentration rises above 10^{18} cm^{-3}, we observe the appearance of the DAP 3 transition at 3.256 eV, which is accompanied by clear emergence of the broadened ABX3 transition in the mid- to high-doping regime. This observation suggests a possible charge transfer from shallowly bound excitons towards the more deeply localized ABX3 center which is further discussed in section V based on PLE spectroscopy results. Similar broadened bound excitonic transitions and dominating DAP luminescences have recently been reported for highly resistive, nitrogen doped ZnO films with doping concentrations above 1×10^{19} cm^{-3}.[35]

Within the scope of this work we will mainly focus on the sample with the lowest Mg concentration of 8×10^{17} cm^{-3} and a dislocation density in the mid 10^9 cm^{-3} regime, since it allows the observation of well resolved donor as well as acceptor related excitation channels for the DAP transitions in PLE spectra. Knowledge of the strain in this sample is essential in order to assure comparability of the results to research on Mg doped GaN grown on, e.g., SiC and GaN substrates, which induce different strain levels in the GaN:Mg layers and hence affects the observable spectral line positions and widths. Based on Raman spectroscopy results, we determine the position of the nonpolar and strain sensitive E^2_{high} Raman mode at 567.3 cm^{-1} that indicates weak compressive strain due to the epitaxial growth on sapphire if compared to the relaxed position of the E^2_{high} Raman mode at 567.0 cm^{-1} in GaN.[36,37] We determine an upper limit for the isotropic biaxial, compressive stress of 0.2 GPa in the sample with a Mg doping of 8×10^{17} cm^{-3} based on uniaxial[38] and hydrostatic Raman deformation potentials.[36]

Figure 2(b) shows the PL spectrum of the sample with a Mg concentration of 8×10^{17} cm^{-3} along with two PLE spectra [see Fig. 2(a)] of the different DAP transitions DAP1 and DAP2, which are not resolvable in the PL spectrum but clearly detectable by PLE due to the appearance of different excitation channels in the spectral regime of the bound excitons. The DAP transition commonly observed in GaN:Mg around 3.28 eV is an overlap of different DAP bands with various chemical and/or structural origins of the participating neutral donors and acceptors. This explains why the splitting between the phonon replica of the merged DAP1 + 2 band does not equal the LO-phonon energy of ∼91 meV for GaN[36,38] but is smaller with ∼87 meV as also observed by Fischer *et al.*[39] in cathodoluminescence spectra. Each DAP band exhibits an individual LO-phonon replica tail that constitutes the different occurring coupling strengths of the LO-phonon interaction due to participation of donors and acceptors with different localization energies. The resulting overlap of the individual LO-phonon replica tails reduces the effectively observed splitting between the corresponding DAP and LO-phonon luminescences in the PL spectra.

For the DAP1 and DAP2, we observe screened excitation channels of the free A and B excitons if compared to the PL transitions FXA and FXB, which is related to the existence of a free exciton surface layer as analyzed in Sec. V. The donor bound excitons DBX1, DBX2 and DBX3 represent excitation channels for the DAP1 and DAP2 with preference for DBX2 as visible in the PLE spectra of Fig. 2. ABX1 appears as the only clearly resolved more deeply bound exciton related excitation channel of DAP1 and is therefore the associated acceptor excitation channel. In contrast, we observe for the DAP2 that ABX2 is the predominant acceptor bound exciton induced excitation channel. Only a weak DAP excitation via the ABX3 is visible in the PLE spectra from Fig. 2 as we observe a rather broad and weak excitation band centered around 3.445 eV. This interpretation of the PLE spectra allows the attribution of the DAP1 to the acceptor bound exciton ABX1 and mainly the donor bound exciton DBX2 and the attribution of the DAP2 to the acceptor bound exciton ABX2 as well as the dominating donor bound exciton DBX2. The additional participation of DBX1 and DBX3 in the excitation process of the DAP luminescence is only accessible via a line shape analysis of the excitation band situated around the energetic position of DBX2, which reveals structured shoulders in the PLE spectra corresponding to the additional minor and not clearly resolved excitation channels as visible in Figs. 2 and 8. Knowledge of the doping concentration, the spectral DAP positions E_{DAP}, and the donor binding energies E^{D}_{bind} allows the determination of the acceptor binding energies E^{A}_{bind} via Eq. (1):[40]

$$E_{\mathrm{DAP}}(N_M) = E_G - \left(E^{A}_{\mathrm{bind}} + E^{D}_{\mathrm{bind}}\right) + \alpha N_M^{1/3}. \qquad (1)$$

The low-temperature (∼2 K) band-gap energy E_G in Eq. (1) can be determined from the position of the free A-Exciton FXA (3.487 eV) in the PL spectrum of Fig. 1 plus the GaN exciton binding energy of ∼25 meV (see Ref. 41) that yields 3.512 eV (see Ref. 42) for E_G. The parameter $\alpha = \sqrt[3]{4\pi/3} \times e^2/(4\pi\epsilon\epsilon_0)$ equals 2.1×10^{-5} meVcm for GaN.[43] However, the majority carrier (electrons) concentration N_M of the analyzed sample with a Mg concentration of 8×10^{17} cm^{-3} can be deduced to be lower than 1×10^{15} cm^{-3} due to the donor background concentration. As a result, the GaN:Mg sample exhibits full compensation of the acceptors as proven by electrical resistivity measurements (not shown) showing high resistivity of the analyzed sample. Hence the Coulomb term $\alpha N_M^{1/3}$ of Eq. (1) can be neglected for the lowly Mg-doped sample as it would result in values <5 meV, which is in the range of the error interval of the acceptor binding energies. Knowledge of the donor binding energy E^{D}_{bind}, which corresponds to the dominating donor bound exciton DBX2, would now allow for determination of the binding energy for all three acceptor bound excitons ABX1, ABX2, and ABX3 via Eq. (1). All donor binding energies will in the following be determined based on a complementary analysis of PLE absorption edges as shown in Fig. 3 and temperature-dependent PL analysis of the DAP luminescence as presented in Fig. 4.

Figure 3 shows the PLE absorption edges for the lowly (8×10^{17} cm^{-3}) Mg-doped sample. The structure of the PLE spectra in close vicinity to the detection energy at DAP1 and

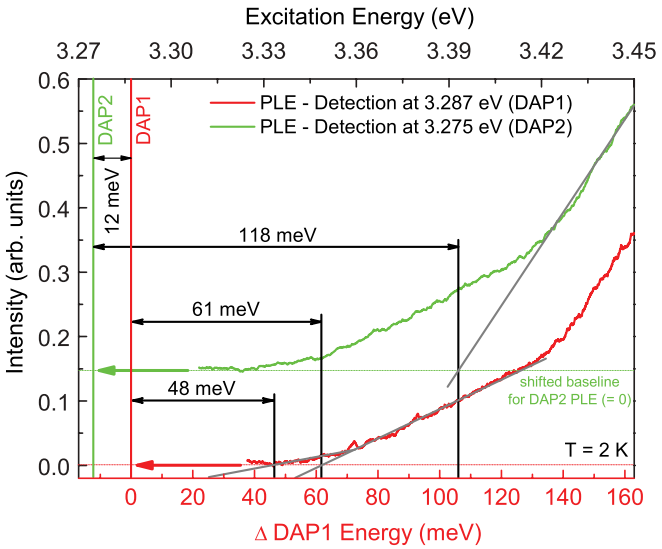

FIG. 3. (Color online) Low-temperature (2 K) PLE spectra of the 8×10^{17} cm^{-3} Mg-doped GaN sample in close energetic vicinity to the DAP1 and DAP2 spectral positions show a structured absorption edge which allows to determine the donor binding energies of the three most prominent donors to 48 ± 5, 61 ± 5, and 118 ± 5 meV by a linear approximation (grey lines). The spectra have been vertically shifted for clarity.

DAP2 allows for a linear extrapolation of the data that results in three different intersection points with the baseline at zero luminescence intensity. Here, the quasiresonant excitation of the DAP luminescence ceases and the energetic difference between the intersection point with the baseline and the detection energy directly provides the donor binding energies of the main participating donors.[21,44,45] Laser excitation with energies below the band-acceptor (e, A) transition energy cannot excite the DAP luminescence. Hence, the energetic difference between the intersection points marked in Fig. 3 and the DAP1 and DAP2 energies results the binding energies for the different involved donor bound excitons DBX1-3. We obtain donor binding energies of 48 ± 5 and 61 ± 5 meV for the shallow donor bound excitons (DBX1, DBX2) and 118 ± 5 meV for the deeper donor bound exciton DBX3.

Absorption spectroscopy yields a trace in absorption spectra of GaN films, which is commonly known as the Urbach tail.[46] This absorption particularity exhibits a biexponential energy dependence for the absorption coefficient in GaN samples of lower structural quality. Jacobson *et al.* conclude that the low energy component of this Urbach tail results from strongly disordered GaN, whereas the high energy component is attributed to the corresponding intrinsic electric field.[47] The PLE spectra from Fig. 3 are possibly influenced by this off-band-edge absorption in GaN but this effect is minor in comparison to the applied linear extrapolation of the PLE spectra for the following three reasons. First, in our high-quality 8×10^{17} cm^{-3} Mg-doped GaN sample, we do not observe an oscillatory structure in the PLE spectra as commonly observed if the energy dependence of the absorption coefficient is measured in lowly doped GaN thin films.[47] Therefore the structure of our PLE spectra is not dominated by the effect of an altering absorption coefficient.

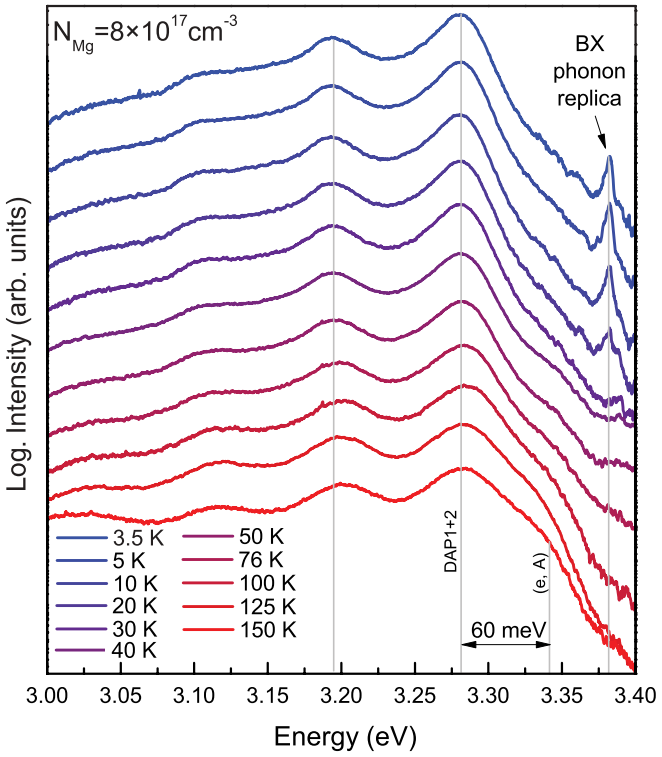

FIG. 4. (Color online) Temperature-resolved PL spectra in the spectral range of the DAP1 + 2 transition measured for the 8×10^{17} cm^{-3} doped GaN:Mg sample. At ∼40 K, the appearance of the (e, A) transition can be observed that coexists with the DAP luminescence at higher temperatures, while thermalization of the LO phonon replica of the bound excitons (BX) occurs. Spectra have been vertically shifted for clarity.

In contrast to absorption spectroscopy, the presented PLE spectra in Fig. 3 show the luminescence signal of the DAP bands and hence analyze excitation and not solely absorption processes. Second, the PLE spectra in Fig. 3 reach zero intensity as soon as the DAP excitation via the band-acceptor (e, A) transitions ceases. This observation stands in contrast to absorption spectra of the low-energy Urbach tail in GaN, which extend down to 3.0 eV in materials of lower quality.[47] Third, the Urbach tail itself scales exponentially as a function of the energy[48] but the PLE spectra from Fig. 3 show a clearly nonexponential relation that allows for the illustrated linear extrapolation.

As origin for DBX1 we favor nitrogen vacancies V_N (see Refs. 32 and 49) or a V_N-H complex[50] in GaN. DBX2 seems to be oxygen related as suggested by SIMS measurements (not shown) that rule out Si as the dominant donor[32] whose bound exciton appears in close energetic vicinity to its oxygen counterpart.[51] The origin of DBX3 is a more controversial case as further discussed in Sec. VII.

Based on temperature-dependent PL spectra as shown in Fig. 4, we can complementarily determine the binding energy of the most prominent donor bound exciton DBX2 in order to support the feasibility of the PLE absorption edge method. Figure 4 shows the DAP1 + 2 luminescence of the 8×10^{17} cm^{-3} Mg-doped GaN sample in a temperature range from 3.5 to 150 K. At ∼40 K, the appearance of the (e, A) transition can be observed[52] due to thermalization of the dominating donor bound exciton DBX2. At 150 K, a clear coexistence of the DAP and the (e, A) luminescence is measured and the energetic difference results in a donor binding energy of 60 ± 5 meV, which is in good agreement with the PLE result of 61 ± 5 meV for DBX2 as deduced based on Fig. 3.

Inserting the value for E_G into Eq. (1) along with the donor binding energy of the most prominent shallow donor bound exciton DBX2 (61 ± 5 meV) now allows the determination of the acceptor binding energies which are associated with the three acceptor bound excitons ABX1, ABX2, and ABX3 and the corresponding DAP1 and DAP2 luminescences. We obtain 164 ± 5 and 176 ± 5 meV for the acceptor binding energies $E_{\text{bind}}^{\text{ABX1}}$ and $E_{\text{bind}}^{\text{ABX2}}$ and corresponding localization energies E_{loc} of 17 ± 2 and 29 ± 2 meV. The later values are directly obtained from the energetic difference between the energetic position of the free A exciton (FXA) and the ABX1 and ABX2 emissions. The determination of the binding energy $E_{\text{bind}}^{\text{ABX3}}$ is based on the line position of DAP3 as it represents the strongest DAP luminescence for samples with Mg doping levels above $\sim 5 \times 10^{18}$ cm^{-3}. The increase of the DAP3 luminescence is accompanied by a strong luminescence enhancement of the ABX3 transition as shown in Fig. 1. Again the most prominent donor DBX2 is applied for the calculation of the acceptor binding energy $E_{\text{bind}}^{\text{ABX3}}$, which yields 195 ± 5 meV and a corresponding localization energy for ABX3 of 42 ± 2 meV. The results of this combined PL, PLE and temperature-dependent PL study are summarized in Table I along with the thermal activation energies E_{act} for ABX1-3 and DBX2-3 as determined in Sec. IV based on temperature dependent PL measurements in the spectral range of the bound excitons.

The proportionality between the localization energy and the respective binding energy for donors and acceptors is known as Haynes's rule[53] and was first established for donors and acceptors in silicon. The corresponding results for the case of the lowly Mg-doped GaN sample are shown in Fig. 5. For the donors, we observe a linear dependence between the localization energy and the binding energy with an inverse slope[53–55] of 0.11, which is in fair agreement with results from Meyer[55] who obtained 0.20 ± 0.01 for the donor bound excitons of a substrate-free and 400-μm-thick GaN film grown by HVPE. However, we obtain a good agreement in regard to the value of 0.12 ± 0.05 as reported by Haynes[53] for the donor bound excitons in silicon as representatives of ideal effective mass like donors. The illustration of DBX3 in Fig. 5 is based on the assumption of a neutral donor bound exciton (D^0X) as the origin of DBX3. Following the results presented in Secs. IV–VI, we will conclude in Sec. VII that DBX3 presents an overlay of an ionized donor bound exciton (D^+X) related to DBX2 as also observed by Šantic *et al.*[56] and a deep donor bound exciton.

The second set of data points in Fig. 5 corresponds to transitions that are related to acceptor states whose linearly approximated dependence exhibits an inverse slope of 0.77. This is in contrast to the result for the donor bound excitons; an observation that supports the attribution of ABX1-3 to acceptor and DBX1-3 to donor bound excitons. The scaling factor between the localization and binding energy for these acceptor states is in contrast to a report of Merz *et al.*[54]

TABLE I. Summary of all analyzed free (FX) and bound excitons (BX) and the donor-acceptor pair (DAP) transitions with their spectral position E_{pos}, their localization energy E_{loc}, their binding energy E_{bind}, and their activation energy E_{act}.

Label	E_{pos} (eV)	E_{loc} (meV)	E_{bind} (meV)	E_{act} (meV)	Origin
FXB	3.495	–	–	–	free B exciton
FXA	3.487	–	–	–	free A exciton
DBX1	3.483	4 ± 2	48 ± 5	–	neutral donor BX, V_N, or V_N-H[a]
DBX2	3.480	7 ± 2	61 ± 5	7.3 ± 0.4	neutral donor BX, oxygen[b]
DBX3	3.474	13 ± 2	118 ± 5	8.0 ± 0.1	overlay of an ionized (DBX2) and a neutral donor BX
ABX1	3.470	17 ± 2	164 ± 5	6.9 ± 0.2	neutral acceptor BX, Mg related shallow transient state[c]
ABX2	3.458	29 ± 2	176 ± 5	4.5 ± 0.2	transitional Mg BX or unknown impurity,[d] see Sec. VII
ABX3	3.445	42 ± 2	195 ± 5	3.6 ± 0.1	neutral acceptor BX, Mg related deep ground state[c]
DAP1	3.287	–	–	–	DAP transition based on DBX2, ABX1 and ABX3
DAP2	3.275	–	–	–	DAP transition based on DBX2, ABX2 and ABX3
DAP3	3.256	–	–	–	DAP transition based on DBX2 and ABX3

[a]References 32,49 and 50.
[b]References 32 and 51.
[c]Reference 26.
[d]References 28,51 and 54.

who obtained 0.1 by taking the acceptor states of Mg and Zn into account. Since ABX1-3 appear upon Mg doping as shown in Fig. 1, we now have the following three main hypotheses for their physical origin: (i) ABX1-3 originate from effective mass like neutral acceptor states along with, e.g., a Mg-complex-related acceptor state.[25] Ionized acceptor states (A^-X) can be excluded due to their instability in GaN based on the electron to hole effective mass ratio that predicts the experimentally proven existence of D^+X.[56] (ii) ABX1, 2, and/or 3 are related to a deep, noneffective mass like Mg acceptor ground state and a shallow, effective mass like Mg transient state as suggested by Lany and Zunger[26] with one ABX of different chemical or structural origin. (iii) ABX1, 2, and/or 3 stem from noneffective mass like defect bound excitons, which can act as donors or acceptors[31] as commonly observed for GaN samples grown on sapphire substrates.[32,51] Application of heteroepitaxy introduces strain fields that support, e.g., the formation of stacking faults[57] and threading dislocations.[51,58] As a result, such complexes can act as donors as well as acceptors and are commonly observed in PL spectra of GaN samples.

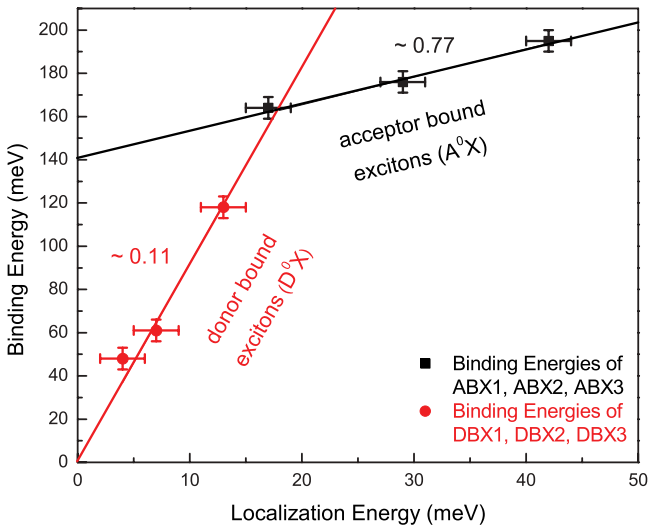

FIG. 5. (Color online) The binding energy as a function of the localization energy yields a linear dependence for the donor and acceptor bound excitons.[53] The proportional constants yield 0.11 for the donor and 0.77 for the acceptor bound excitons.

In the following, we will analyze these main three hypotheses. Points (i) and (ii) are analyzed in Sec. V by PLE spectroscopy, which can reveal transfer processes between free excitonic and donor- as well as acceptor-bound excitonic states. The influence of defect bound excitons from point (iii) is analyzed based on their thermalization behavior as presented in Sec. IV and the related decay dynamics as shown in Sec. VI. Defect bound excitons with large localization energies exhibit smaller decay times and rapid thermalization upon temperature increase in PL studies if compared to impurity bound excitons as, e.g., observed by Wagner *et al.* in ZnO.[31] As a result, we will then conclude with the final interpretation of our data in Secs. VII and VIII.

IV. DETERMINATION OF THE ACTIVATION ENERGIES

Temperature-resolved PL spectroscopy is a viable tool for detecting noneffective mass like centers such as defect and complex bound excitons, which were suggested in Sec. III as possible origin of the observed BX emission lines. Figure 6 shows a temperature -dependent series of PL spectra of the 8×10^{17} cm^{-3} doped GaN:Mg sample in the spectral range of the free and bound excitons that directly adjoints to the spectral range in Fig. 4. First, it should be noted that no dominant emission from deeply bound and structural defect-related excitons is visible as commonly reported for heteroepitaxially grown GaN films.[32,51] Separating free excitonic emission from bound excitonic emission is enabled by their different thermalization behavior[31] as displayed in Fig. 6. While the free A-exciton emission FXA gains in intensity with increasing temperature the bound excitons DBX2, DBX3, and ABX1-3 thermalize as apparent by their drastic intensity loss. Emission of DBX1 cannot be observed in the presented series of temperature dependent PL spectra. Furthermore, the energetic

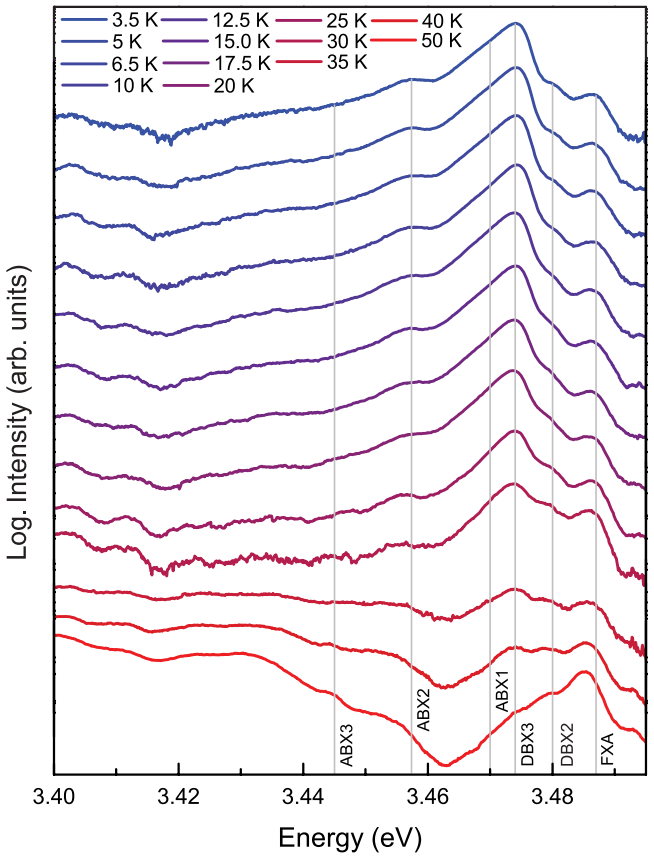

FIG. 6. (Color online) Temperature-resolved PL spectra of the bound (ABX1-3, DBX2-3) and free (FXA) excitons of the 8×10^{17} cm^{-3} doped GaN:Mg sample. Spectra have been vertically shifted for clarity.

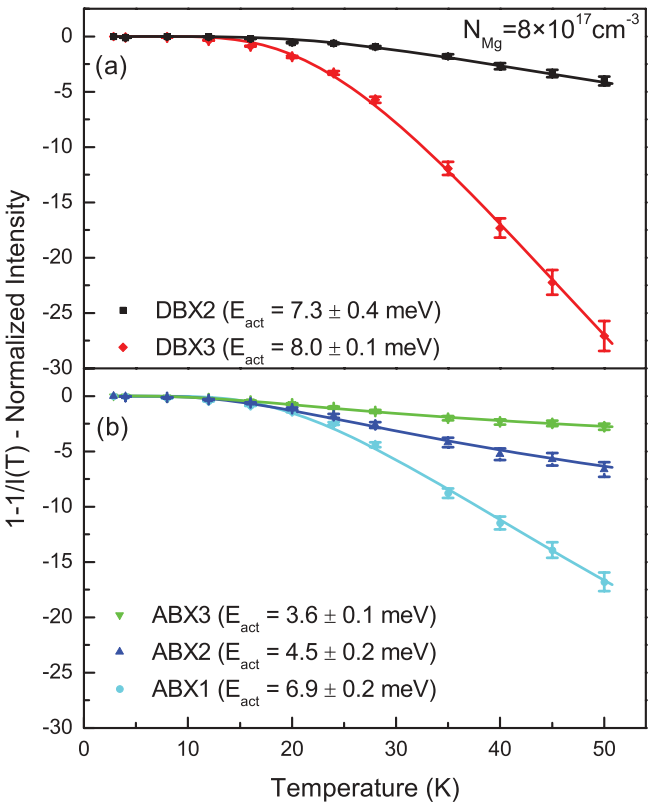

FIG. 7. (Color online) Intensity of the donor bound excitons DBX2-3 (a) and the acceptor bound excitons ABX1-3 (b) over a temperature range from 3–50 K. The resulting activation energy E_{act} is a measure of the thermalization process. Numbers in parentheses represent the errors.

position of the FXA transition clearly follows the thermally induced energetic reduction of the band gap which is, e.g., described by the empirical Varshni model[59] or, in more detail, is modeled by Vina *et al.*[60,61] who apply the Bose-Einstein model and obtained a more reliable description for lower temperatures. The bound excitons in GaN also experience such a redshift of their luminescences but due to their localization this effect is weaker[34,54,55] and cannot clearly be resolved in the analyzed temperature window for a GaN:Mg sample with spectral linewidths of ∼5 meV. However, the different evolution of the intensity and the spectral position of the bound and free excitonic transitions still allows their identification.

If the absolute intensities of the DBX2-3 and ABX1-3 transitions in Fig. 6 are plotted against the temperature, then the activation energies E_{act} of the different centers can be determined as shown in Fig. 7. As a simplistic approach, the decreasing luminescence intensity of bound excitons can be described by a three-step process. First, the bound excitons thermalize into their excited states in the low-temperature regime ($\lesssim$20 K).[62–64] This process is followed by the complete detachment of the excitons from their binding complexes in the mid-temperature regime ($\lesssim$50 K)[65,66] as mainly considered in Fig. 7. Finally, hole and electron thermalization into antibinding acceptor or donor states takes place at elevated temperatures ($\gtrsim$50 K).[32,63,65] All these three thermalization process categories are commonly accompanied by an increasing redistribution of the thermalized carriers among unquenched, deeper radiation channels[65] as also, e.g., clearly visible in Fig. 6 in the temperature range between 30–50 K below the energetic position of the ABX3. In order to compare the thermalization behavior of donor and acceptor bound excitons in the mid-temperature regime ($\lesssim$50 K), we normalized the peak intensities and fitted the data with a single exponential dissociation process as described by Eq. (2):[62]

$$I(T) = 1/(1 + ce^{-E_{act}/kT}). \quad (2)$$

The results of the fitting procedure based on Eq. (2) are represented by the solid lines in Fig. 7 and are listed in Table I. Only the data points up to 50 K were included because the thermal shift of the FXA and FXB transition towards the bound excitons increasingly falsifies the determination of the peak intensities at higher temperatures. Due to the poor luminescence intensity of the ABX3 transition in the 8×10^{17} cm^{-3} doped GaN:Mg sample, we included the corresponding data from the thermal dissociation behavior of a higher doped (7×10^{18} cm^{-3}) GaN:Mg sample and included it in Fig. 7(b) for the comparison of the thermal quenching behavior. For a more careful analysis of the three-step dissociation process,[62,65] it would be necessary to evaluate the crucial temperature range in reasonably small temperature steps on a sample with sufficiently small spectral linewidths, which is beyond the scope of the presented work. Figure 7 mainly serves for the identification of, e.g., defect

bound excitons, which should exhibit drastic discontinuities in the evolution of E_{act} as a function of E_{loc}.[31,32] For the dominating donor bound exciton DBX2. we observe $E_{act} = 8.0 \pm 0.1$ meV, which is in good agreement with $E_{loc} = 7 \pm 2$ meV from Table I. The deeper localized center DBX3 ($E_{loc} = 13 \pm 2$ meV) exhibits a larger E_{act} of 8.0 ± 0.1 meV, which describes the more rapid thermalization of DBX3. A similar thermalization behavior for DBX2 and DBX3 has been observed by Šantic *et al.*[56] in nominally undoped and moderately Mg doped (4×10^{17} cm^{-3}–2×10^{18} cm^{-3}) GaN and suggests the attribution of DBX3 to the ionized donor bound exciton D^+X, which directly corresponds to the neutral state DBX2 (D^0X). Interestingly, we observe an opposite scaling of E_{act} for ABX1-3 over the corresponding E_{loc} (see Table I). This effect could originate from carrier redistribution of dissociated excitons at shallow centers towards the deeper ABX states,[65] which means that the measured intensity for deeper centers strongly depends on the thermalization level of the remaining luminescence channels. However, also the temperature dependence of capture cross sections needs to be taken into account, which further leads to the apparent differences between the actual thermal depth of the center, E_{loc} and E_{act} (see Table I).[65,66] As E_{act} of the deeper ABX1-3 transitions continuously scales with the corresponding E_{loc} we can, as a first approach, exclude defect bound excitons such as Y-lines as their origin, which are commonly observed in the same energetic regime.[32] Wagner *et al.*[31] have shown that deeply localized Y-lines in ZnO thermalize more rapidly than more shallowly localized D^0X. We cannot observe such behavior for our GaN:Mg sample and will further support our given interpretation by time-resolved measurements in Sec. VI.

V. TRANSFER PROCESSES

Figure 8(a) compares the PLE spectra of DAP1 and DAP2 from Fig. 2(a) with selected PLE spectra of ABX3, ABX2, DBX3, and DBX2 on a logarithmic intensity scale. The donor bound exciton DBX2 exhibits a PLE spectrum that clearly shows the FXB (3.495 eV) and FXA (3.487 eV) as excitation channels corresponding to maxima in the PLE spectrum and the PL spectrum in Fig. 2(b). After the laser excitation, the generated free excitons are transferred towards the bound exciton related binding centers and are spatially localized via a fast capturing process as discussed in Sec. VI. The exciton transfer process towards DBX3 is also shown in Fig. 8, which again exhibits FXB and FXA as main, but less well resolved excitation channels, similar to what is observed for ABX1 (not shown) and ABX2. With decreasing detection energies of these centers, transfer process between the bound excitons start to hinder the observation of well resolved excitation channels due to a PL and PLE linewidth of ∼5 meV. However, for the rather broad ABX3 transition which strongly appears in GaN:Mg samples with Mg concentrations of above 2×10^{18} cm^{-3} as shown in Fig. 1, we observe an excitation channel at 3.463 eV, which is 18 ± 2 meV higher in energy compared to its corresponding luminescence. We can exclude an ionized acceptor state (A^-X) as origin for this excitation channel due to its instability in GaN based on the electron to hole effective mass ratio.[56]

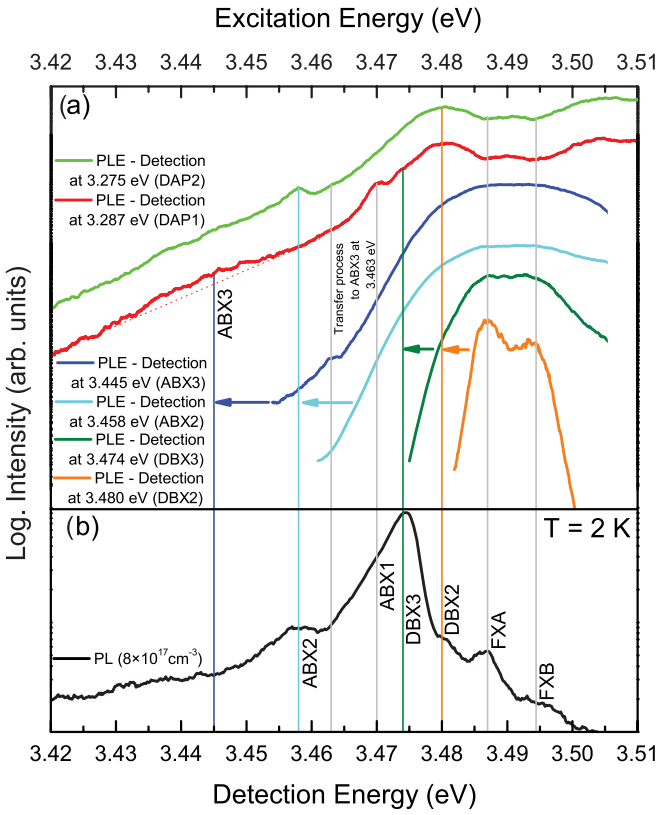

FIG. 8. (Color online) PL and PLE spectra of the 8×10^{17} cm^{-3} Mg-doped GaN sample in the spectral range of the free (FX) and bound (DBX, ABX) excitons. The drop lines indicate the detection energy. Spectra have been vertically shifted for clarity.

Generally, excitation resonances of bound excitons can be divided into groups according to the different excitation mechanisms.[31,64,67] Participation of rotational and vibrational states is observed in the group with the smallest energy distance to the detection energy (1–2 meV), which cannot be resolved in our samples with PLE linewidths of ∼5 meV. The next group of excitation channels involves acceptor bound excitons with holes from valence bands that lie energetically below the A-valence band as, e.g., observed for structural defect bound excitons in ZnO.[31] Based on Table I, we observe an A-B-valence band splitting of 8 ± 2 meV, which is in good agreement with reported results[55,68] but well below the observed energetic gap of 18 ± 2 meV between ABX3 and its excitation channel. Suggestively, the A-C-valence band splitting amounts to ∼18–20 meV in GaN.[55,68] However, excitation of ABX3 via acceptor states binding an exciton, which comprises a hole from the C-valence band, should be minor due to the low temperature (2 K).[31,55,67] The observation of corresponding excitation channels for ABX1 and ABX2 is hindered by the spectral overlap with the donor bound exciton excitation channels and hence we cannot exclude C-valence band related excitation of ABX3. The third group of excitation channels are the electronic excited states of the exciton, which can well reach energy spacings greater than, e.g., the A-B-valence band splitting in GaN and can be theoretically modeled following a formalism presented by Puls *et al.*[69] for exciton complexes in CdS. We assume that excitonic complexes with orbital (radial) n_r and angular momentum

quantum number l in the range of $0 \leqslant (n_r,l) \leqslant 2$ are viable candidates for the observed excitation channel of ABX3 but the linewidth limitations of the excitation channels hinders a more detailed analysis.

The bound exciton related excitation channels in the PLE spectra of DAP1 and DAP2 are represented by maxima in Fig. 8(a) that appear at identical spectral position as their PL counterparts. However, for the free excitons, we observe in Figs. 2(a) and 8(a) that the resonances in the PLE spectra of DAP1 and DAP2 appear as shifted towards higher energies if compared to the corresponding peaks in the PL spectra [see Fig. 8(b)]. Careful analysis of Fig. 8 shows that the luminescence maxima of FXA and FXB correspond to minima in the PLE spectra; an effect that was already, e.g., observed by Broser *et al.*[21] for the case of CdS. Both, free and bound excitons cause strong absorption in the GaN:Mg crystal and hence their corresponding laser-induced luminescences originate from a comparably thin surface layer. However, a DAP luminescence originates more from the bulk of a crystal where neutral donors and acceptors are present. These donors and acceptors are either directly generated due to the laser excitation or stem from a dissociation of bound excitons. Generally, a, e.g., neutral acceptor bound exciton represents a three-particle system, which suffices (neglecting the energy balance) to neutralize one ionized donor state and two ionized acceptor states following its dissociation and charge transport of the electron and the holes towards ionized donors and acceptors in the close vicinity, respectively. While such ionized acceptor states are unstable in GaN,[56] they must still participate in the generation process of neutral donor and acceptor states.[70] Hence the bound exciton dissociation generates additional neutral donor and acceptor states, which enhance the DAP luminescence when the electron and holes on the neutral donor and acceptor sites recombine radiatively by returning to equilibrium via $D^0X + A^0X \rightarrow \hbar\omega + D^+X + A^-X$ with a following rapid dissociation or neutralization of the unstable A^-X complex. This process is directly mirrored by resonances in the PLE spectrum at the energetic position where luminescence of bound excitons occurs as shown in Fig. 8.

However, free excitonic absorption in GaN is so strong that a thin free exciton surface layer is formed that efficiently absorbs the DAP luminescences[21] by dissociation of the free excitons. Timusk *et al.* describe the particular infrared absorption of free excitons in Si and Ge but also show the extension of this absorption towards the free excitonic continuum[71,72] that originates the observed DAP absorption at significantly larger energies. This process is clearly measurable by the minima in the PLE spectra at the maxima of the free excitonic luminescences. Generally, free excitons dissociate nonradiatively and are subsequently captured at impurities, which then form neutral acceptors and donors. This nonradiatively dissociation strengthens the DAP luminescences but the whole effect is strongly overcompensated by the absorption of the DAP luminescence originating from the bulk of the crystal in the free exciton surface layer. This explanation also allows to understand why maxima can be seen in the PLE spectra of the DAP on the high-energy side of the corresponding FXA and FXB luminescence. Due to the detuning of the excitation energy the free exciton concentration decreases in the free exciton surface layer, which consequently allows the exciting light to further penetrate into the bulk where free excitons can be generated. These free excitons support the formation of neutral donors and acceptors, which, in turn, strengthens the DAP luminescence. The resulting peak in the DAP excitation spectra is further enhanced by the reduced DAP luminescence absorption in the weakly established free exciton surface layer. The combination of both processes explains why maxima can be seen in the PLE spectra of DAPs on the high-energy side of the corresponding PL luminescences.

VI. DYNAMICS OF THE BOUND EXCITONS

In general, the lifetimes of excitonic transitions represent a measure for the crystal quality of the samples.[73] In high-quality HVPE GaN samples with low donor background concentrations ($<1 \times 10^{16}$ cm^{-3}) a comparably long biexponential decay for, e.g., excitons bound to the oxygen donor is observed with time constants of $\tau_{D1} = 0.28$ ns and $\tau_{D2} = 1.1$ ns at 2 K.[74] Epitaxially grown GaN films exhibit donor bound exciton lifetimes with fast τ_{D1} components of, e.g., 60 to 110 ps whose values scale with the biaxial stress present in such samples.[51,75]

Figure 9(a) shows two representative transients of the acceptor bound exciton ABX1 and the donor bound exciton DBX3. Such decaying behavior as summarized for the donor bound excitons DBX2 and DBX3 and the acceptor bound excitons ABX1, ABX2, and ABX3 in Fig. 9(b) is well described by a biexponential decay function after deconvolution of the luminescence signal with the response function of the time resolved PL setup. DBX1 could not spectrally be resolved under pulsed excitation in PL spectra. The fast decay component τ_{D1} for the two donors yields 115 ± 15 and 125 ± 15 ps, whereas values between 90 ± 15 ps and 115 ± 15 ps are observed for τ_{A1} of the acceptors ABX1, ABX2, and ABX3. The longer second exponential decay component for the donors τ_{D2} yields 635 ± 15 ps and 710 ± 15

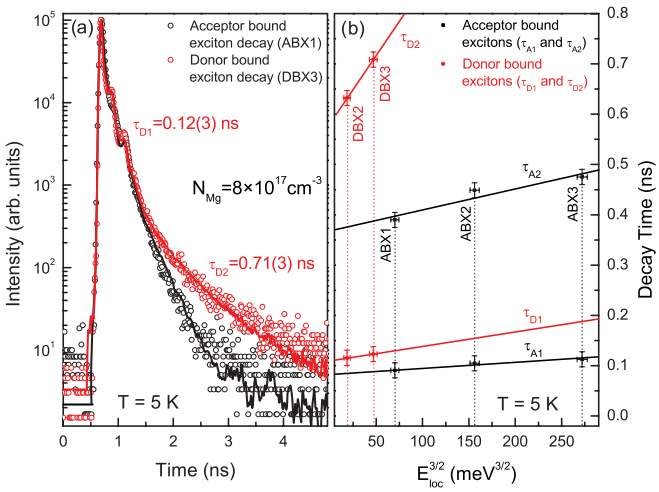

FIG. 9. (Color online) (a) Transients of the bound excitons ABX1 and DBX3. Solid lines show the response function deconvoluted data. (b) Lifetimes $\tau_{D1,A1}$ and $\tau_{D2,A2}$ of DBX2, DBX3, ABX1-3 as a function of the localization energy $E_{\mathrm{loc}}^{3/2}$. Solid lines represent fits based on a model by Rashba and Gurgenishvili[76] and numbers in parentheses represent the errors.

ps and τ_{A2} scales between 395 ± 15 and 480 ± 15 ps for the acceptor bound excitons. The biexponential decay indicates that a second decay channel must be present in addition to the purely excitonic decay channel of the recombination of the bound excitons. The observation of the second longer lifetime $\tau_{D2,A2}$ is facilitated by the saturation of, e.g., a nonradiative capture process, which is characterized by a faster time constant τ_{cap}.[66,77] The fast decay times $\tau_{D1,A1}$, which represent the decay shortly after the excitation can therefore be described by a combination of the actual excitonic recombination τ_{rec} and the time constant τ_{cap} accounting for the dynamics of the capturing process as denoted in Eq. (3):

$$1/\tau_{D1,A1} = 1/\tau_{\text{rec}} + 1/\tau_{\text{cap}}. \tag{3}$$

Therefore $\tau_{D2,A2}$ equals to τ_{rec} and the intensity ratio of $\sim$1:1000 of the decay amplitudes that correspond to $\tau_{D1,A1}$ and $\tau_{D2,A2}$ demonstrates that capture process clearly dominate the temporal luminescence behavior of the epitaxially grown GaN:Mg film. However, already the observation of the slower time component $\tau_{D2,A2}$ accounts for the quality of the analyzed sample and assures the observation of PLE excitation channels in Sec. V. The absence of a resolvable rise time in the transients of the 8×10^{17} cm^{-3} doped GaN:Mg sample along with a monoexponential decay time for the free A-exciton FXA of $\sim$60 ps (not shown) suggests that the transfer process of free excitons towards binding centers as measured by PLE is immediately saturated and subsequently dominated by a capturing process of the free excitons towards deeper centers. Based on a model by Rashba and Gurgenishvili,[76,78] the lifetime of a bound exciton is proportional to $E_{\text{loc}}^{3/2}$, which can qualitatively be deduced considering the inverse proportionality between the oscillator strength f of a bound exciton and its radiative lifetime τ.[79] The oscillator strength f of a bound exciton is determined by the spatial extend of the region that is occupied by the electron-hole complex as described by the Bohr radius a_{BX} of the bound excitons and the total number of corresponding impurities.[80] Hence these radii a_{BX} are proportional to the localization energy E_{loc} for centers that bind the exciton as a hole quasiparticle ($a_{BX} \propto 1/\sqrt{E_{\text{loc}}}$). As a result, we can deduce the following set of proportions:

$$\tau \propto 1/f \propto 1/a_{BX}^3 \propto E_{\text{loc}}^{3/2}. \tag{4}$$

Figure 9(b) suggests that Eq. (4) holds for both time constants $\tau_{D1,A1}$ and $\tau_{D2,A2}$ even though the limited number of data points prevents more detailed proof for the E_{loc} dependence. However, it can be seen that the slope of the fit to the data in Fig. 9(b) is always smaller for the faster decay (τ_{D1} and τ_{A1}) component if compared to the corresponding larger time constants $\tau_{D2,A2}$ as also observed for the case of bound excitons in ZnO by Wagner *et al.*[31] Furthermore, the slope of the fit to the data seems to be larger for the donor bound excitons if compared to the acceptor bound excitons due to the larger general localization energy of the latter which supports the assignment of these bound excitons to be either donor or acceptor bound. Also, we do not observe lifetimes that violate the presented E_{loc} dependence as observed for the Y-lines in ZnO,[31] so we can exclude the appearance of structural defect bound excitons and suggest that DBX2-3 and ABX1-3 originate from impurity bound excitons.

VII. DISCUSSION

In Sec. III, we outlined three different hypotheses (i)–(iii) for the origin of ABX1-3. Approach (i) would interpret ABX1-3 as excitons bound to effective mass like neutral acceptor states in combination with, e.g., a Mg-H complex related acceptor state. We exclude the observation of complex related acceptor states as, e.g., described by Gelhausen *et al.*,[81] and further authors[15,16,24] as we observe stable emission from all bound excitonic emission lines under UV illumination due to complete activation of the lowly Mg-doped (8×10^{17} cm^{-3}) GaN sample. Emission from acceptor complex related bound excitons is not radiation hard under UV illumination and hence leads to an alteration of the PL spectra on a time scale of minutes.[24,25] Also complex bound excitons as, e.g., excitons bound to extended structural defect complexes[31] exhibit drastically different luminescence lifetimes if compared to their point defectlike and impurity-related counterparts; an effect which is not observed as shown in Sec. VI. All the observed lifetimes scale with their attributed localization energy as $E_{\text{loc}}^{3/2}$.[76] Furthermore, defect bound excitons exhibit strongly different thermal activation energies E_{act} if compared to point defect bound excitons in their close energetic vicinity[31,64] but in Sec. IV and Table I, it is shown that E_{act} scales with E_{loc} without the occurrence of such structural defect bound exciton related particularities.[31] It was found that E_{act} of the donor bound excitons (DBX2, DBX3) directly scales with the related E_{loc} as listed in Table I. In contrast, a decrease of E_{act} with rising E_{loc} is observed for the acceptor bound excitons ABX1-3 that can be explained by charge carrier transfer from thermalized shallow donor bound excitons towards more deeply localized acceptor bound excitons.[65] Hence, the combination of temperature-dependent and time-resolved PL measurements from Secs. IV and VI allows us to exclude points (i) and (iii) as interpretation possibilities for the observed PL spectra.

Based on an experimental work of Monemar *et al.*[25] and the theoretical approach by Lany *et al.*,[26] we interpret our data following point (ii). ABX1 is an effective mass like shallow transient Mg_{Ga} state (STS) with an acceptor binding energy of 164 ± 5 meV, which is in good agreement with theoretical results of Lany *et al.* based on DFT calculations using the projector augmented wave method yielding 150 meV.[26] Furthermore, the theoretical approach predicts a lattice-relaxed, noneffective mass like Mg_{Ga} deep ground state (DGS) with an acceptor binding energy of 180 meV,[26] which we observe as ABX3 with an acceptor binding energy of 195 ± 5 meV. Even though we observe an offset between the absolute values of the acceptor binding energies, we obtain an acceptor binding energy difference of 31 meV, which is in excellent agreement with the theoretically determined difference of 30 meV. Interestingly, we observe ABX3 in Figs. 2 and 8 as a rather broad luminescence and excitation band that can be understood based on the results of Lany *et al.*[26,28] who describe the corresponding DGS acceptor wave function as strongly localized at single N atoms in contrast to the highly symmetric STS configuration. Such strong spatial localization of noneffective mass like acceptor wave functions causes vulnerability to local strain field variations in the GaN crystal, which is directly mirrored by the broader luminescence and excitation band of ABX3. Furthermore, the theoretical model of Lany *et al.* predicts

the observation of the ABX1 related STS in *n*-type samples, whereas the DGS (ABX3) should mainly be observable in *p*-type specimen due to different occurring carrier lifetimes[26] and a transfer process between STS and DGS. We observe both optical transitions related to STS and DGS in our highly resistive sample, which further motivates the selection of a GaN:Mg sample with a Mg concentration of 8×10^{17} cm^{-3} for the conducted luminescence analysis. Figure 1 clearly shows that an increasing Mg concentration and hence hole concentration is accompanied by an optical activation of the deeper ABX states due to more efficient transfer processes between the STS and the DGS related energy levels. Lany *et al.* estimated an energy barrier between the STS and the DGS of down to 20 meV, which facilities interstate transfer processes on the time scale of the PL lifetimes.[26] Hence, the intensity ratio of ABX1 and ABX3 as synonymic for the STS and the DGS could represent a practical tool for an estimation of the GaN sample's hole concentration; a method that accounts for all wurtzite materials which exhibit a similar dual nature of the acceptor states as, e.g., CdS[1] and ZnO.[28]

The role of the acceptor bound exciton ABX2 remains controversial as it could either represent a transitional, partially lattice relaxed Mg_{Ga} state between the STS and the DGS or an acceptor bound exciton with different chemical identity as, e.g., Zn[51,54] or Be.[28] Figure 5 results a proportionality factor of 0.77 between the acceptor binding energies E_{bind} and the corresponding localization energies E_{loc} of the ABX1-3. This is in clear contrast to results from Merz *et al.* who considered one Mg- and one Zn-bound exciton state in their analysis and obtained a value of 0.1. Hence the discrepancy could result from a partly identical chemical origin for the binding centers of the acceptor bound excitons ABX1-3, which is not in accordance with the original assumption of Haynes[53] but still results in the presented linear dependence between E_{bind} and E_{loc} from Fig. 5. A similarly controversial case is represented by the observed DBX3 transition which could either constitute an additional shallow neutral acceptor (A^0X), a deep neutral donor (D^0X), or an ionized donor bound exciton (D^+X). The analysis of the lifetimes in Sec. VI clearly separates the donor and acceptor bound excitons based on the observed lifetimes $\tau_{D1,A1}$ and $\tau_{D2,A2}$, which is further supported by the determined activation energies E_{act} from Sec. IV. Hence DBX3 is either a deep neutral donor and/or an ionized donor bound exciton. Figure 7(a) exhibits a rather fast thermalization behavior of DBX3 ($E_{\text{act}} = 8.0 \pm 0.1$ meV) in comparison to DBX2 ($E_{\text{act}} = 7.3 \pm 0.4$ meV), which has also been observed by Šantic *et al.*[56] in nominally undoped and moderately Mg-doped (4×10^{17} cm^{-3}–2×10^{18} cm^{-3}) GaN. This allows the assignment of DBX3 to a D^+X, which corresponds to the neutral bound exciton state DBX2 (D^0X). Thereby the splitting between the DBX3 and DBX2 transition of 6 ± 2 meV agrees well with the result of Šantic *et al.* who determined 5.5 ± 5 meV.[56] Furthermore, the D^+X (DBX3) transition exhibits strong LO-phonon interaction[56] as shown in Fig. 2 for DBX3 and ABX1. We determine a Huang-Rhys-Factor (HRF) of $S = 0.072 \pm 0.003$ for DBX3 and $S = 0.138 \pm 0.003$ for ABX1, while no LO-phonon replica of, e.g., FXA or DBX2 can be separated from the luminescence background in the PL spectra of the lowly Mg (8×10^{17} cm^{-3}) or not intentionally doped GaN sample. Determination of such large HRFs further excludes the observation of defect bound excitons as suggested in point (iii), which exhibit approximately one order of magnitude lower values[31] for the HRF. Even though DBX3 is identified as the ionized donor bound exciton (D^+X) of the neutral donor bound exciton (D^0X) DBX2, we have further indications for a more complex interpretation of DBX3 which also justifies plotting DBX3 in Fig. 5 under the assumption of Haynes rule.[53] DBX3 appears in Figs. 5 and 9 as an overlay of a deep neutral donor bound exciton and the ionized donor bound exciton (D^+X) corresponding to DBX2. Generally, the ionized states of donor bound excitons appear as well pronounced excitation channels in PLE spectra[64] but Fig. 8 only reveals a weak excitation channel at the spectral position of DBX2 in the low-energy flank of the PLE spectrum of DBX3. Furthermore, Bertram *et al.*[77] have observed shorter values for τ_{D1} of ionized donor bound excitons (D^+X) compared to τ_{D1} of their neutral equivalents D^0X, which is in clear contrast to the case of DBX2 and DBX3 where the lifetimes τ_{D1} and τ_{D2} increase with E_{loc} as shown in Fig. 9. Hence we assume an overlay of the D^+X state related to DBX2 (D^0X) and a deep donor bound exciton with unknown chemical origin as origin for the total observed DBX3 luminescence. This interpretation is further supported by the PLE spectra of Figs. 2 and 8, which show that DBX2 is the main DAP excitation channel which dominates the excitation channel via DBX3. A similar efficient DAP excitation should be observable in PLE spectra if the DBX3 luminescence would purely originate from ionized donor bound excitons (D^+X) related to the neutral D^0X center (DBX2). This argumentation favors the interpretation of an overlay of the D^+X luminescence with the luminescence of a deep donor at 3.474 eV.

Interestingly, we observe maxima at the energetic positions of the free excitons FXA and FXB in the PLE spectra of bound excitons as, e.g., DBX2 (see Fig. 8) but minima at the same energetic positions in the PLE spectra of the DAP luminescences (see Figs. 2 and 8). As discussed in Sec. V, this observation proves the existence of a thin free exciton surface layer in our lowly (8×10^{17} cm^{-3}) Mg-doped GaN sample. Comparable observations were reported for CdS,[21] which generally indicates a good crystal quality as no defect- and/or dopant-related binding centers seem to efficiently trap the generated free excitons. The PLE spectrum of ABX3 in Fig. 8 reveals an excitation channel that lies 18 ± 2 meV higher in energy and does not energetically match with any of the observed bound excitonic transitions. In Sec. V, we suggested that the observed excitation channel represents the excitation of the DGS via an electronic excited state of the exciton as, e.g., observed by Meyer *et al.*[64] for the case of donor bound excitons in ZnO. No transfer process as suggested by Lany *et al.*[26] between the STS and the DGS (ABX1 and ABX3) was measurable by PLE spectroscopy as shown in Fig. 8. Hence we suggest that the energy transfer between the two Mg_{Ga} states takes place via the excited states of the DGS transition (ABX3), which could not clearly be resolved for our sample with PL and PLE linewidth of ∼5 meV. The final proof remains a task for future PLE work on, e.g., doped bulk GaN:Mg samples with up to an order of magnitude lower emission linewidth.[51,82]

Regarding a recent publication by Lyons *et al.*,[27] we would like to remark that none of our Mg-doped samples as shown

in Fig. 8 exhibits any strong, so-called blue luminescence centered at either 2.7 or 2.8 eV (not shown), even though some samples exhibit Mg concentrations ($1–2 \times 10^{19}$ cm^{-3}), which already facilitate *p* conductivity. Indeed, we already observe a broad luminescence background centered around 3.0 eV for our unintentionally doped GaN sample as partially shown in Fig. 1 but it is two orders of magnitude weaker in intensity than the bound excitonic luminescence or the DAP luminescence of lowly intentionally Mg-doped GaN. Furthermore, the DAP1 and DAP2 emissions at 3.287 and 3.275 eV of the lowly Mg-doped (8×10^{17} cm^{-3}) sample are stable under UV light excitation along with their corresponding bound excitonic emissions and hence an originating Mg-H complex seems unlikely[27] as we fully thermally activated our samples. The DAP1 and DAP2 transition exhibit all typical characteristics of DAP transitions as exemplarily shown in this work by PLE spectroscopy (see Figs. 2, 3, and 8) and temperature-dependent PL (see Fig. 4). The temperature dependence shows the transition from the DAP to the (e, A) luminescence due to thermalization of the most prominent donor DBX2 in very good accordance to the PLE results from Sec. III. Furthermore, the good agreement between the determined acceptor binding energies for ABX1 and ABX3 (164 ± 5 and 195 ± 5 meV) and the theoretical approach by Lany *et al.*[26] stands in clear contrast to the recently described model for the Mg_{Ga} state by Lyons *et al.*[27] We cannot confirm the therein presented Mg-H origin for the luminescences at 3.27 eV nor the proposed direct relation between the blue luminescence at 2.7–2.8 eV and a deep Mg_{Ga} acceptor level. A detailed comparison of the two opposing models of Lyons *et al.*,[27] and Lany *et al.*[26] based on a combined luminescence study with focus on the blue and the DAP luminescence remains a task for future work.

VIII. CONCLUSION

In summary, we have interpreted the signature of Mg doping in the PL signal of lowly Mg-doped (8×10^{17} cm^{-3}) and technologically most relevant MOCVD grown GaN on sapphire substrates and summarized all derived values as, e.g., binding E_{bind}, localization E_{loc} and thermal activation energies E_{act} in Table I. It was shown by photoluminescence excitation (PLE) spectroscopy that the commonly observed donor-acceptor pair (DAP) luminescences at 3.287 eV (DAP1) and 3.275 eV (DAP2) are both most dominantly excited via free excitons of the A- and B-valence band and the oxygen donor (DBX2). Interestingly, for the latter case, the DBX2 neutral donor bound exciton does not represent the strongest signal in the PL spectra of the bound excitons, which are commonly applied for studying the effect of Mg doping in GaN. Hence, only PLE spectroscopy allows for the attribution of the main three acceptor bound exciton related luminescences (ABX1-3) along with the dominating donor bound exciton (DBX2) to their corresponding DAP luminescences. We identified two Mg_{Ga} related acceptor states in our samples that correspond to a deeply localized, noneffective mass like ground state and a shallow, effective mass like transient state whose intensity ratio scales with the carrier concentration and hence represents a viable tool for analyzing *p* doping in GaN:Mg. The combined study of PLE excitation channels in the energetic vicinity of the DAP luminescences enabled the determination of the binding energies of the three mainly involved donors in our GaN:Mg sample (48 ± 5, 61 ± 5, and 118 ± 5 meV). Temperature-resolved PL spectroscopy further demonstrated the transition from the DAP luminescence to the band acceptor (e, A) luminescence, which yielded the donor binding energy of the oxygen donor bound exciton in accordance with the PLE results. Based on a combined temperature-dependent and time-resolved PL study, we excluded the observation of deeply localized structural defect bound excitons and showed consistent scaling of E_{act} and the observed time constants $\tau_{D1,A1}$ and $\tau_{D2,A2}$ with E_{loc} of the mainly observed donor and acceptor bound excitons. As a main result, we determined three acceptor binding energies (164 ± 5, 176 ± 5, and 195 ± 5 meV) based on the presented combination of luminescence techniques that correspond to a dual Mg_{Ga} related acceptor state and an additional impurity or transitional Mg acceptor state. Such a dual nature of acceptor states appears as a general phenomenon in wide-band-gap materials and has already been reported for ZnO:Li[83] and CdS.[1] Analysis of the transfer processes between all main donor and acceptor bound excitons by PLE spectroscopy has revealed an excited state of the deeply localized, noneffective mass like Mg_{Ga} ground state, which is 18 ± 2 meV higher in energy and has furthermore supported the finding of an ionized donor bound exciton, which is related to the common neutral oxygen donor in GaN.

ACKNOWLEDGMENTS

This work was supported by the DFG within grant No. SFB787 and the NSF within grant No. 1108071.

*callsen@tu-berlin.de

[1] B. Gil, P. Bigenwald, P. P. Paskov, and B. Monemar, Phys. Rev. B **81**, 085211 (2010).
[2] D. G. Thomas and J. J. Hopfield, Phys. Rev. **128**, 2135 (1962).
[3] R. Baumert, I. Broser, J. Gutowski, and A. Hoffmann, Phys. Rev. B **27**, 6263 (1983).
[4] J. Qiu, J. M. Depuydt, H. Cheng, and M. Haase, Appl. Phys. Lett. **59**, 2992 (1991).
[5] A. Zeuner, H. Alves, D. M. Hofmann, B. K. Meyer, A. Hoffmann, U. Haboeck, M. Strassburg, and M. Dworzak, Phys. Status Solidi B-Basic Solid State Physics **234**, R7 (2002).
[6] S. Lautenschlaeger, S. Eisermann, B. K. Meyer, G. Callsen, M. R. Wagner, and A. Hoffmann, Phys. Status Solidi-Rapid Res. Lett. **3**, 16 (2009).
[7] S. Lautenschlaeger, M. Hofmann, S. Eisermann, G. Haas, M. Pinnisch, A. Laufer, and B. K. Meyer, Phys. Status Solidi B **248**, 1217 (2011).
[8] H. Amano, M. Kito, K. Hiramatsu, and I. Akasaki, Jpn. J. Appl. Phys. **28**, L2112 (1989).

[9]S. Yoshida, S. Misawa, and S. Gonda, Appl. Phys. Lett. **42**, 427 (1983).
[10]F. Ponce and D. Bour, Nature (London) **386**, 351 (1997).
[11]S. Nakamura, M. Senoh, S. Nagahama, N. Iwasa, T. Yamada, T. Matsushita, H. Kiyoku, and Y. Sugimoto, Jpn. J. Appl. Phys. Part 2-Lett. **35**, L217 (1996).
[12]S. Nakamura, M. Senoh, S. Nagahama, N. Iwasa, T. Yamada, T. Matsushita, H. Kiyoku, and Y. Sugimoto, Jpn. J. Appl. Phys. Part 2-Lett. **35**, L74 (1996).
[13]I. Akasaki, H. Amano, M. Kito, and K. Hiramatsu, J. Lumin. **48-49**, 666 (1991).
[14]S. Nakamura, T. Mukai, M. Senoh, and N. Iwasa, Jpn. J. Appl. Phys. Part 2-Lett. **31**, L139 (1992).
[15]Y. Kamiura, Y. Yamashita, and S. Nakamura, Jpn. J. Appl. Phys. Part 2-Lett. **37**, L970 (1998).
[16]Y. Kamiura, Y. Yamashita, and S. Nakamura, Physica B-Condens. Matter **273**, 54 (1999).
[17]M. Godlewski, H. Przybylinska, R. Bozek, E. Goldys, J. Bergman, B. Monemar, I. Grzegory, and S. Porowski, Phys. Status Solidi A **201**, 216 (2004).
[18]A. Hoffmann, A. Kaschner, and C. Thomsen, Phys. Status Solidi C **6**, 1783 (2003).
[19]P. Bäume, J. Gutowski, D. Wiesmann, R. Heitz, A. Hoffmann, E. Kurtz, D. Hommel, and G. Landwehr, Appl. Phys. Lett. **67**, 1914 (1995).
[20]R. Heitz, E. Moll, V. Kutzer, D. Wiesmann, B. Lummer, A. Hoffmann, I. Broser, P. Bäume, W. Taudt, J. Sollner, and M. Heuken, J. Cryst. Growth **159**, 307 (1996).
[21]I. Broser, J. Gutowski, and R. Riedel, Solid State Commun. **49**, 445 (1984).
[22]L. Eckey, U. von Gfug, J. Holst, A. Hoffmann, A. Kaschner, H. Siegle, C. Thomsen, B. Schineller, K. Heime, M. Heuken, O. Schon, and R. Beccard, J. Appl. Phys. **84**, 5828 (1998).
[23]U. Kaufmann, P. Schlotter, H. Obloh, K. Kohler, and M. Maier, Phys. Rev. B **62**, 10867 (2000).
[24]G. Pozina, C. Hemmingsson, P. P. Paskov, J. P. Bergman, B. Monemar, T. Kawashima, H. Amano, I. Akasaki, and A. Usui, Appl. Phys. Lett. **92**, 151904 (2008).
[25]B. Monemar, P. P. Paskov, G. Pozina, C. Hemmingsson, J. P. Bergman, T. Kawashima, H. Amano, I. Akasaki, T. Paskova, S. Figge, D. Hommel, and A. Usui, Phys. Rev. Lett. **102**, 235501 (2009).
[26]S. Lany and A. Zunger, Appl. Phys. Lett. **96**, 142114 (2010).
[27]J. L. Lyons, A. Janotti, and C. G. Van de Walle, Phys. Rev. Lett. **108**, 156403 (2012).
[28]S. Lany and A. Zunger, Phys. Rev. B **80**, 085202 (2009).
[29]E. R. Glaser, W. E. Carlos, G. C. B. Braga, J. A. Freitas, W. J. Moore, B. V. Shanabrook, R. L. Henry, A. E. Wickenden, D. D. Koleske, H. Obloh, P. Kozodoy, S. P. DenBaars, and U. K. Mishra, Phys. Rev. B **65**, 085312 (2002).
[30]E. Glaser, M. Murthy, J. Freitas, Jr, D. Storm, L. Zhou, and D. Smith, Physica B-Condens. Matter **401**, 327 (2007).
[31]M. R. Wagner, G. Callsen, J. S. Reparaz, J. H. Schulze, R. Kirste, M. Cobet, I. Ostapenko, S. Rodt, C. Nenstiel, M. Kaiser, A. Hoffmann, A. V. Rodina, M. R. Phillips, S. Lautenschlaeger, S. Eisermann, and B. K. Meyer, Phys. Rev. B **84**, 035313 (2011).
[32]M. A. Reshchikov and H. Morkoç, J. Appl. Phys. **97**, 061301 (2005).
[33]S. Mita, R. Collazo, A. Rice, R. Dalmau, and Z. Sitar, J. Appl. Phys. **104**, 013521 (2008).
[34]B. Monemar, P. P. Paskov, J. P. Bergman, A. A. Toropov, T. V. Shubina, S. Figge, T. Paskova, D. Hommel, A. Usui, M. Iwaya, S. Kamiyama, H. Amano, and I. Akasaki, Mat. Sci. Semicon. Proc. **9**, 168 (2006).
[35]S. Lautenschlaeger, S. Eisermann, G. Haas, E. A. Zolnowski, M. N. Hofmann, A. Laufer, M. Pinnisch, B. K. Meyer, M. R. Wagner, J. S. Reparaz, G. Callsen, A. Hoffmann, A. Chernikov, S. Chatterjee, V. Bornwasser, and M. Koch, Phys. Rev. B **85**, 235204 (2012).
[36]A. R. Goni, H. Siegle, K. Syassen, C. Thomsen, and J. M. Wagner, Phys. Rev. B **64**, 035205 (2001).
[37]U. Haboeck, H. Siegle, A. Hoffmann, and C. Thomsen, Phys. Status Solidi C, 1710 (2003).
[38]G. Callsen, J. S. Reparaz, M. R. Wagner, R. Kirste, C. Nenstiel, A. Hoffmann, and M. R. Phillips, Appl. Phys. Lett. **98**, 061906 (2011).
[39]A. M. Fischer, S. Srinivasan, F. A. Ponce, B. Monemar, F. Bertram, and J. Christen, Appl. Phys. Lett. **93**, 151901 (2008).
[40]D. G. Thomas, J. J. Hopfield, and W. M. Augustyniak, Phys. Rev. **140**, A202 (1965).
[41]S. Xu, W. Liu, and M. Li, Appl. Phys. Lett. **81**, 2959 (2002).
[42]B. Monemar, J. Bergman, I. Buyanova, H. Amano, I. Akasaki, T. Detchprohm, K. Hiramatsu, and N. Sawaki, Solid-State Electron. **41**, 239 (1997).
[43]B. K. Meyer, D. Volm, A. Graber, H. C. Alt, T. Detchprohm, A. Amano, and I. Akasaki, Solid State Commun. **95**, 597 (1995).
[44]I. Broser, D. Pathe, and M. Rosenzweig, Solid State Commun. **54**, 849 (1985).
[45]E. Reuter, R. Zhang, T. Kuech, and S. Bishop, MRS Internet J. Nitride Semicond. Res. **4**, G3.67 (1999).
[46]F. Urbach, Phys. Rev. **92**, 1324 (1953).
[47]M. A. Jacobson, O. V. Konstantinov, D. K. Nelson, S. O. Romanovskii, and Z. Hatzopoulos, J. Cryst. Growth **230**, 459 (2001).
[48]S. Chichibu, T. Mizutani, T. Shioda, H. Nakanishi, T. Deguchi, T. Azuhata, T. Sota, and S. Nakamura, Appl. Phys. Lett. **70**, 3440 (1997).
[49]Q. Yang, H. Feick, and E. Weber, Appl. Phys. Lett. **82**, 3002 (2003).
[50]D. G. Chtchekine, Z. C. Feng, G. D. Gilliland, S. J. Chua, and D. Wolford, Phys. Rev. B **60**, 15980 (1999).
[51]B. Monemar, J. Phys.: Condens. Matter **13**, 7011 (2001).
[52]S. Fischer, C. Wetzel, E. E. Haller, and B. K. Meyer, Appl. Phys. Lett. **67**, 1298 (1995).
[53]J. Haynes, Phys. Rev. Lett. **4**, 361 (1960).
[54]C. Merz, M. Kunzer, U. Kaufmann, I. Akasaki, and H. Amano, Semicond. Sci. Technol. **11**, 712 (1996).
[55]B. K. Meyer, MRS Proc. **449**, 497 (1997).
[56]B. Šantic, C. Merz, U. Kaufmann, R. Niebuhr, H. Obloh, and K. Bachem, Appl. Phys. Lett. **71**, 1837 (1997).
[57]G. Pozina, P. P. Paskov, J. P. Bergman, C. Hemmingsson, L. Hultman, B. Monemar, H. Amano, I. Akasaki, and A. Usui, Appl. Phys. Lett. **91**, 221901 (2007).
[58]J. Xie, S. Mita, A. Rice, J. Tweedie, L. Hussey, R. Collazo, and Z. Sitar, Appl. Phys. Lett. **98**, 202101 (2011).
[59]Y. Varshni, Physica **34**, 149 (1967).
[60]K. Odonnell and X. Chen, Appl. Phys. Lett. **58**, 2924 (1991).

[61]L. Vinna, S. Logothetidis, and M. Cardona, Phys. Rev. B **30**, 1979 (1984).
[62]D. Bimberg, M. Sondergeld, and E. Grobe, Phys. Rev. B **4**, 3451 (1971).
[63]C. Henry and K. Nassau, Phys. Rev. B **2**, 997 (1970).
[64]B. K. Meyer, J. Sann, S. Eisermann, S. Lautenschlaeger, M. R. Wagner, M. Kaiser, G. Callsen, J. S. Reparaz, and A. Hoffmann, Phys. Rev. B **82**, 115207 (2010).
[65]M. A. Reshchikov and R. Y. Korotkov, Phys. Rev. B **64**, 115205 (2001).
[66]O. Brandt, J. Ringling, K. H. Ploog, H. J. Wünsche, and F. Henneberger, Phys. Rev. B **58**, 15977 (1998).
[67]J. Gutowski, N. Presser, and I. Broser, Phys. Rev. B **38**, 9746 (1988).
[68]B. Monemar, Phys. Rev. B **10**, 676 (1974).
[69]J. Puls, F. Henneberger, and J. Voigt, Phys. Status Solidi B **119**, 291 (1983).
[70]J. J. Hopfield, in *Proceedings of the Seventh International Conference Physics of Semiconductors, 1964* (Academic, New York, 1964), p. 725.
[71]T. Timusk, Phys. Rev. B **13**, 3511 (1976).
[72]T. Timusk, H. Navarro, N. O. Lipari, and M. Altarelli, Solid State Commun. **25**, 217 (1978).
[73]T. Koida, S. Chichibu, A. Uedono, A. Tsukazaki, M. Kawasaki, T. Sota, Y. Segawa, and H. Koinuma, Appl. Phys. Lett. **82**, 532 (2003).
[74]B. Monemar, P. P. Paskov, J. P. Bergman, G. Pozina, A. A. Toropov, T. V. Shubina, T. Malinauskas, and A. Usui, Phys. Rev. B **82**, 235202 (2010).
[75]G. Pozina, N. Edwards, J. Bergman, B. Monemar, M. Bremser, and R. Davis, Phys. Status Solidi A **183**, 151 (2001).
[76]E. I. Rashba and G. E. Gurgenishvili, Sov. Phys. Solid State **4**, 759 (1962).
[77]F. Bertram, J. Christen, A. Dadgar, and A. Krost, Appl. Phys. Lett. **90**, 041917 (2007).
[78]E. I. Rashba, Sov. Phys. Semicond. USSR **8**, 807 (1975).
[79]G. W. 'tHooft, W. A. J. A. Van DerPoel, L. W. Molenkamp, and C. T. Foxon, Phys. Rev. B **35**, 8281 (1987).
[80]T. V. Shubina, M. M. Glazov, A. A. Toropov, N. A. Gippius, A. Vasson, J. Leymarie, A. Kavokin, A. Usui, J. P. Bergman, G. Pozina, and B. Monemar, Phys. Rev. Lett. **100**, 087402 (2008).
[81]O. Gelhausen, M. R. Phillips, E. M. Goldys, T. Paskova, B. Monemar, M. Strassburg, and A. Hoffmann, Phys. Rev. B **69**, 125210 (2004).
[82]B. Monemar, P. P. Paskov, J. P. Bergman, A. A. Toropov, T. V. Shubina, T. Malinauskas, and A. Usui, Phys. Status Solidi B **245**, 1723 (2008).
[83]B. Meyer, J. Stehr, A. Hofstaetter, N. Volbers, A. Zeuner, and J. Sann, Appl. Phys. A **88**, 119 (2007).